

Scientific Report

Concerning the implementation of the project: January – December 2012

For this study, cobalt oxide was electrochemically obtained on boron-doped polycrystalline diamond films (deposited on Si wafers by means of microwave plasma-assisted chemical vapor deposition) by a straightforward method, previously described in detail. Briefly, Co_3O_4 was deposited at an applied potential of 1.45 V vs. Ag/AgCl electrode from a 0.25 M NaHCO_3 aqueous solution containing 2 mM $\text{Co}(\text{NO}_3)_2$, and the oxide loading was controlled by appropriately adjusting the deposition time. Oxide-modified BDD electrodes were then used as substrate for platinum cathodic deposition, carried out from a 1 M NaOH and 4.8 mM H_2PtCl_6 solution, at an applied potential of -0.7 V. The same method was employed for platinum deposition on bare BDD, and the electrodes thus obtained were also used, for comparison. During Pt(IV) reduction, the cathodic current was recorded in order to calculate the corresponding deposition electric charge. For a reliable estimation of the Pt loading, prior to platinum deposition chronoamperometric curves were recorded under the same experimental conditions in the background electrolyte. The deposition charge was then calculated as the difference between the cathodic charge in the presence of Pt(IV) salt and that recorded in its absence.

It is worthwhile to note that in order to investigate the effect of the Co_3O_4 substrate on the electrochemical behavior of the deposited Pt particles a continuous oxide film is obviously better suited than a deposit consisting of isolated particles or clusters. In the present work, for further platinum deposition, oxide-modified BDD electrodes with Γ_{Co} values within the range 30 to 90 nmol cm^{-2} were used as substrates. This is because, as the

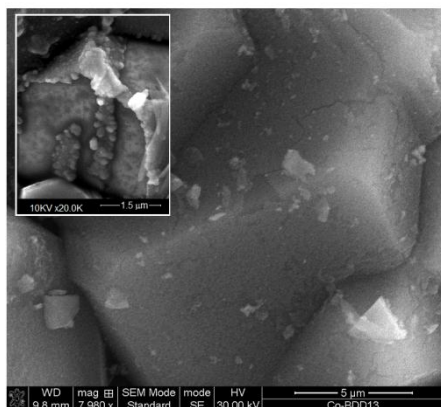


Fig. 1 SEM image of a cobalt oxide layer electrochemically deposited on BDD (surface concentration of cobalt sites, $\Gamma_{\text{Co}} = 40.7 \text{ nmol cm}^{-2}$). Inset: micrograph of a BDD/Pt electrode with $\Gamma_{\text{Co}} = 15.6 \text{ nmol cm}^{-2}$

results of the EIS measurements indicate, such oxide loadings allow obtaining rather continuous films with reasonably good resistivity (from *ca.* 5 to *ca.* 22 ohm cm^2).

Fig. 1 shows a typical SEM image obtained after the stabilization of the voltammetric response for a cobalt oxide-coated BDD electrode ($\text{Co}_3\text{O}_4/\text{BDD}$) with a surface concentration of cobalt sites of 40.7 nmol cm^{-2} . It can be observed that the BDD surface is covered by a more or less continuous oxide layer of rather uniform thickness, although some cracks are also evident, mainly on the edges and at the boundaries of the diamond crystallites. Nevertheless, in the context of the present work this is not a matter of concern because the surface area of bare diamond exposed to the solution is very small and, due to the

specific features of BDD (extremely low double layer capacitance and inertness to adsorption), its contribution to the electrochemical behavior of the $\text{Co}_3\text{O}_4/\text{BDD}$ electrodes can be neglected. SEM measurements also showed that for Γ_{Co} values lower than *ca.* 20 nmol cm^{-2} the oxide layer is still discontinuous, as illustrated by the micrograph from the inset in Fig. 1.

In order to assess the possibility of electrochemically obtaining $\text{Co}_3\text{O}_4\text{-Pt}$ composite materials oxide-modified BDD electrodes were further used as substrate for Pt electrochemical deposition, and the behavior of the electrodes thus obtained

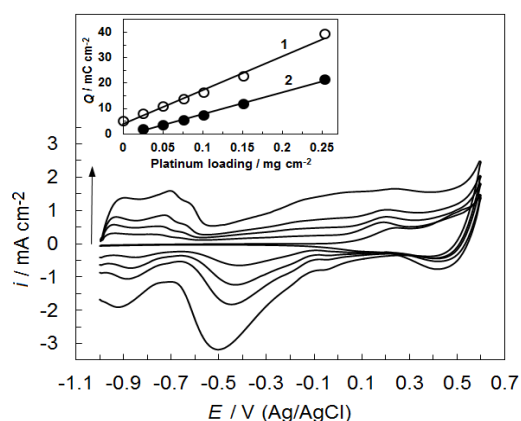


Fig. 2 Cyclic voltammograms recorded in 1 M NaOH (sweep rate, 50 mV s^{-1}) for $\text{Pt}/\text{Co}_3\text{O}_4/\text{BDD}$ electrodes. Γ_{Co} : $30.2 \text{ nmol cm}^{-2}$. Pt loading (mg cm^{-2}): 0; 0.050; 0.101; 0.152; 0.253 (arrow indicates increasing Pt loading). Inset: the effect of Pt loading on the voltammetric charge integrated for $\text{Pt}/\text{Co}_3\text{O}_4/\text{BDD}$ (1) and Pt/BDD (2) electrodes

($\text{Pt}/\text{Co}_3\text{O}_4/\text{BDD}$) was firstly checked by cyclic voltammetry. Fig. 2 shows characteristic voltammetric patterns obtained in alkaline media for $\text{Pt}/\text{Co}_3\text{O}_4/\text{BDD}$ electrodes with platinum loading ranging from 0 to 0.253 mg cm^{-2} . The most obvious result of the platinum deposition is the significant enhancement of the potential range corresponding to a rather uniform distribution of the voltammetric charge. We should note that this behavior could have some implications for electrochemical capacitor applications because, as voltammograms from Fig. 2 indicate, the use of Pt-modified cobalt oxide coatings could enable, at least in principle, a working voltage of *ca.* 1.55 V (from -1.00 to 0.55 V), much higher than that available without platinum modification (*ca.* 0.65 V, from -0.1 to 0.55 V).

It was also found that the voltammetric charge (integrated as the average of the anodic and cathodic charges within the potential range from -1 to 0.55 V) exhibited by $\text{Pt}/\text{Co}_3\text{O}_4/\text{BDD}$ electrodes linearly increases (slope 133 mC mg^{-1} , $R^2=0.9899$) with the platinum loading (see curve 1 from the inset in Fig. 2). To better put into evidence the role of the Co_3O_4 substrate, electrodes obtained by platinum electrodeposition on bare conductive diamond (Pt/BDD) were also used, for comparison. As curve 2 from the inset in Fig. 2 shows, for Pt/BDD electrodes the voltammetric charge (calculated as above) is also linearly increasing with the platinum loading, although the regression statistical analysis yielded a lower slope (86 mC mg^{-1} with $R^2=0.9969$).

The electrochemically active surface area of the platinum deposit can be estimated from the charge associated with hydrogen adsorption, corrected for that for the double layer. Thus, from the cyclic voltammograms in Fig.2, integration of the cathodic charge within the potential range -1.0 to -0.7 V resulted in an average value of the hydrogen adsorption charge of *ca.* $9.77 \text{ mC mg}^{-1} \text{ Pt}$. By assuming a value of 0.21 mC cm^{-2} for a smooth platinum surface [38], a specific surface area of *ca.* $4.65 \text{ m}^2 \text{ g}^{-1}$ can be roughly estimated for the Pt particles

deposited on the Co_3O_4 ($\Gamma_{\text{Co}}=30.2 \text{ nmol cm}^{-2}$) substrate. These findings are noteworthy because they indicate that the use of a cobalt oxide substrate for Pt deposition enables more efficient use of the noble metal in terms of electrochemically active specific surface area, most likely due to a better dispersion and/or to a smaller size of the Pt particles.

The stability of the electrochemically deposited composites was appraised by cyclic voltammetry, within the potential range -1.0 to 0.6 V in a 1M NaOH solution at a sweep rate of 50 mV s^{-1} , and Fig. 3 shows the effect of 50 consecutive voltammetric runs performed (after previous stabilization) with a Pt/ Co_3O_4 /BDD ($\Gamma_{\text{Co}}=80.7 \text{ nmol cm}^{-2}$, Pt loading, 0.230 mg cm^{-2}) electrode. Based upon the charge

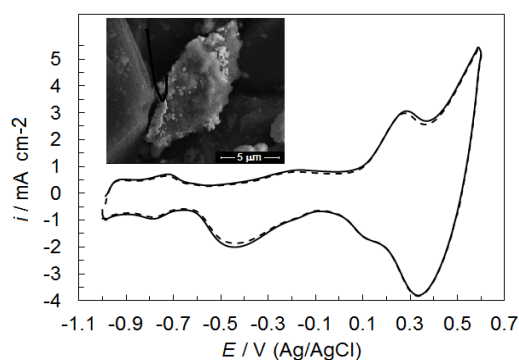


Fig. 3 Voltammograms recorded in 1 M NaOH during consecutive cycles (sweep rate, 50 mV s^{-1}) for Pt/ Co_3O_4 /BDD electrodes. Solid line, first cycle; dashed line cycle 50. Γ_{Co} , $80.7 \text{ nmol cm}^{-2}$. Pt loading, 0.230 mg cm^{-2} . Inset: SEM micrograph of the electrode

a specific capacitance of 431 F cm^{-3} can be calculated for the electrochemically obtained Co_3O_4 -Pt composite. This value compares well with the capacitance of 391.6 F cm^{-3} (available in acidic media, within the potential range 0.0 to 1.0 V vs. Ag/AgCl) reported for

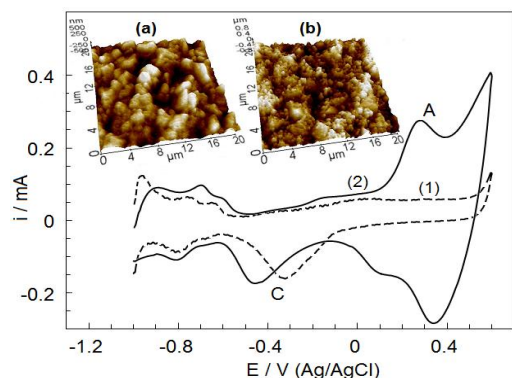


Fig. 4 Voltammograms in 1 M NaOH for Pt/BDD (1) and Pt/ Co_3O_4 /BDD (2). Insets: AFM images of Pt/BDD (a) and Pt/ Co_3O_4 /BDD (b). Γ_{Co} : 38 nmol cm^{-2} . Pt loading (mg cm^{-2}): (1), 0.037; (2), 0.038.

integrated from the cyclic voltammogram in Fig. 3 (within the potential range -1.0 to 0.55 V), an initial value of the capacitance of 28.01 mF cm^{-2} was calculated and it was observed that after 50 consecutive cycles (see dashed curve) this value decreased with only *ca.* 4.3% (down to 26.81 mF cm^{-2}), indicating a good stability of the composite deposit from the BDD surface.

In order to better put these results into perspective, we should note that, from SEM micrographs (see for example the inset in Fig. 3), the thickness of the composite deposit from the above electrodes was estimated to be of *ca.* $0.65 \mu\text{m}$. By taking into account the value of *ca.* 28 mF cm^{-2} obtained from cyclic voltammograms, a specific capacitance of 431 F cm^{-3} can be calculated for the electrochemically obtained Co_3O_4 -Pt composites electrodes obtained by a RF magnetron co-sputtering method.

The promising features of Co_3O_4 -Pt composites, electrochemically deposited on boron-doped diamond, prompted us to investigate methanol oxidation at Pt/ Co_3O_4 /BDD electrodes, with an eye towards the effect of the Co_3O_4 substrate on the resistance to fouling of the Pt particles. Fig. 4 shows typical voltammograms recorded in alkaline media for Pt/BDD and Pt/ Co_3O_4 /BDD, together with the AFM topological images of the electrodes.

Compared to bare BDD, the Co_3O_4 substrate allows a more uniform distribution and a smaller average size of the deposited Pt particles. Statistical analysis of the AFM results yielded root mean square roughness values of *ca.* 195 nm and 230 nm for Pt/BDD and Pt/ Co_3O_4 /BDD, respectively. The higher roughness of the composite is in line with the increase of the capacitive-like background current evidenced by the voltammograms from Fig. 4. The same feature results in an enhanced electrochemically active surface area of the platinum from the Pt- Co_3O_4 composite. Thus, from Fig. 4, areas of Pt particles of *ca.* $6.6 \text{ m}^2 \text{ g}^{-1}$ and $7.5 \text{ m}^2 \text{ g}^{-1}$ were calculated for Pt/BDD and Pt/ Co_3O_4 /BDD, respectively, by integrating the corresponding cathodic charge associated with hydrogen adsorption and by assuming a value of 0.2 mC cm^{-2} for smooth platinum. It appeared that for Pt/ Co_3O_4 /BDD the peak corresponding to platinum oxides reduction (labeled B) is cathodically shifted with *ca.* 150 mV, indicating a higher stability of Pt oxide species in the composite. In the present work the methanol oxidation current was always normalized to the active surface area of the Pt deposits, estimated as above.

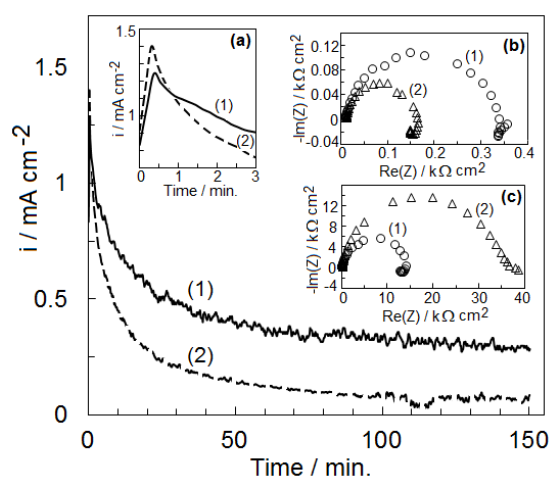


Fig. 5 Chronoamperograms for methanol oxidation at Pt/ Co_3O_4 /BDD (1) and Pt/BDD (2). Insets show initial part of the curves (a), and EIS results before (b) and after prolonged methanol oxidation (c) for Pt/ Co_3O_4 /BDD (1) and Pt/BDD (2). Solution: 1 M NaOH + 2.46 M CH_3OH .

0.3 V) at Pt/ Co_3O_4 /BDD (1) and Pt/BDD (2), both before (inset b) and after long-time polarization measurements (inset c). Before prolonged electrolysis, a lower charge-transfer resistance was observed at Pt/BDD, in line with the higher oxidation current recorded in the initial part of the chronoamperogram. This behavior suggests that the presence of Co_3O_4 hinders to some extent the access of the methanol to the active sites of the electrocatalyst, probably due to the higher roughness of the composite. For the two types of electrodes, continuous methanol oxidation leads to an increase of both real and imaginary parts of the impedance, indicating some blockage of the Pt particles surface by adsorbed CO. Nevertheless, the deleterious effect of this process on the activity for methanol oxidation

The activity was also checked by long-term polarization measurements in 1 M NaOH + 2.46 M CH_3OH solution at an applied potential of -0.3 V, and Fig. 5 shows typical results. In the early stage of the electrolysis (inset a), the current was higher when the platinum was deposited on bare BDD. However, after 150 min of continuous polarization, the oxidation current at Pt/ Co_3O_4 /BDD electrodes reached $\sim 22\%$ of its initial value, while that for the Pt/BDD decreased to $\sim 6\%$. This is an indication that during methanol oxidation in alkaline media platinum is less sensitive to deactivation (*e.g.*, via CO poisoning) when deposited on Co_3O_4 substrate, compared to Pt on bare BDD. Insets in Fig. 5 show Nyquist plots recorded (in freshly prepared solutions, at -

(estimated from the ratio of the charge-transfer resistances before and after electrolysis) is more marked for Pt on bare BDD. Thus, after 150 min of electrolysis, the charge-transfer resistance at Pt/BDD exceeds by far that observed for Pt/Co₃O₄/BDD, which is further proof of the increased resistance to fouling of Co₃O₄-supported Pt particles.

A two-step electrochemical procedure was also employed in order to obtain Pt-TiO₂ composite layers on the electrodes surface. First, hydrated titanium oxide was electrodeposited on the working electrodes (BDD or GC) surface by anodic hydrolysis of TiCl₃, according to a method previously described in the literature. Briefly, a constant

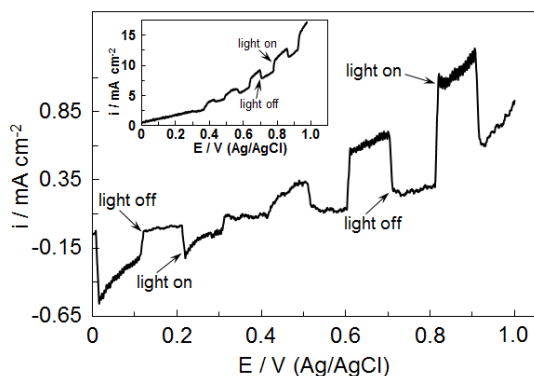


Fig. 6 Current-potential dependence upon intermittent UV illumination for a TiO₂/BDD electrode. Inset: same dependence for a TiO₂/GC electrode. TiO₂ deposition charge, 230 mC cm⁻²; electrolyte, 0.1 M KCl; scan rate, 10 mV s⁻¹.

potential (0.6 V) was applied to the electrode in an aqueous solution (pH 2.0) containing 50 mM TiCl₃ and 0.1 M KCl, and the oxide loading was controlled by appropriate adjustment of the deposition charge. In the second step of the procedure, the electrodes were immersed in a 0.5 M H₂SO₄ + 2.5 mM H₂PtCl₆ solution, and platinum deposition was carried out potentiostatically (applied potential, -0.1 V). The amount of deposited Pt was then calculated from the corresponding cathodic charge (estimated from chronoamperometric curves recorded both in the absence and in the presence of the platinum precursor). For comparison, the same procedure was used for platinum electrodeposition on bare BDD.

The photoelectrochemical activity of the TiO₂/BDD electrodes obtained as above was examined in 0.1 M KCl electrolyte using a UV mercury lamp. Fig. 6 shows the photocurrent obtained for chopped illuminated conditions on this electrode system, while sweeping the potential from 0 to 1 V with a scan rate of 10 mV s⁻¹. It should be noted that both cathodic and anodic photocurrents were observed and there are reasons to believe that the cathodic photocurrent could be due to the BDD support which is a p-type semiconductor. It is reasonable to ascribe the anodic photocurrent to the presence of the TiO₂, since for bare BDD under the same experimental conditions no significant photoanodic current was observed. In order to put these results into a better perspective, the inset in Fig. 6 illustrates the results of the same experiment performed with a TiO₂/GC electrode with same oxide loading. The BDD surface is hydrogen-terminated and highly homogenous in structure which ensures complete coverage with TiO₂ films, even for low oxide loadings. This feature, together with the extremely low background current and the high overpotential for oxygen evolution of the conductive diamond result in the much lower dark current recorded at the TiO₂/BDD electrodes. These results are also noteworthy because they suggest that for

photoelectrocatalytic applications BDD is a much better substrate for TiO_2 , in terms of efficient separation of the photoinduced charge carriers. Thus, as Fig. 6 shows, at an applied potential of 0.7 V, the current recorded at TiO_2/GC upon irradiation is only *ca.* 1.2 times higher than the dark value, whereas, at the TiO_2/BDD electrode the light to dark current ratio was found to be *ca.* 2.6. A reasonable explanation for this behavior is provided by assuming that the oxygen-containing groups that are usually present at the edge plane surface of sp^2 carbonaceous supports could partially trap the photogenerated charge carriers. Conversely, BDD films are obviously free of such oxygen-containing groups because, due to the obtaining conditions (chemical vapor deposition in hydrogen plasma) their surface is inherently hydrogen-terminated.

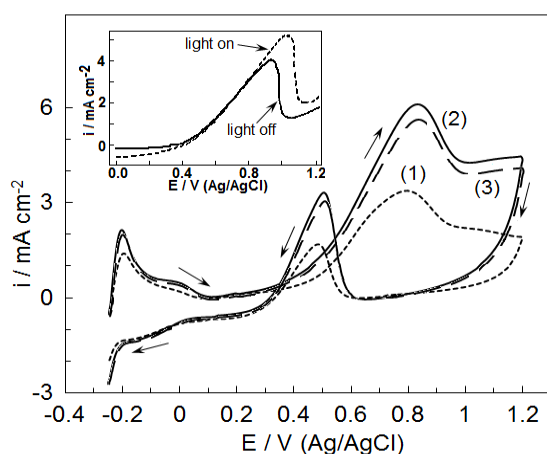


Fig. 7 Cyclic voltammograms in a 0.5 M H_2SO_4 + 1 M CH_3OH solution during the 5th scan at Pt/BDD (1) and during the 5th and 65th scans at Pt/ TiO_2 /BDD electrodes (2 and 3, respectively). Inset: linear sweep voltammograms at the Pt/ TiO_2 /BDD electrode in dark (solid line) and under UV illumination (dotted line). Scan rate, 5 mV s^{-1} .

of Pt particles evidenced by SEM), although some catalytic effect of the TiO_2 substrate cannot be completely ruled out. Nevertheless, this is an issue that remains to be addressed. The stability of the Pt/ TiO_2 /BDD electrodes during methanol oxidation was appraised by performing several consecutive voltammetric cycles under the same experimental conditions as above. As curve 3 from Fig. 7 shows, 60 more runs resulted in a rather small decrease of the main peak current (*ca.* 8.5 %). It is also interesting to note that the voltammetric response seems to be affected only within the potential range that corresponds to the oxidation of the methanol (*i.e.* at potential values higher than *ca.* 0.3 V). This behavior suggests that the decrease of the oxidation current is due to a partial deactivation (probably by CO poisoning) of the Pt particles surface, rather than to a loss of noble metal from the electrode.

The photocatalytic activity of the Pt/ TiO_2 /BDD electrodes was also checked and the inset in Fig. 7 shows linear sweep voltammograms recorded at low scan rate (5 mV s^{-1}) in the same methanol-containing solution, both in dark and under UV illumination. The

In order to assess the electrocatalytic activity of the composite, methanol anodic oxidation was used again as a test-reaction and Fig. 7 illustrates the voltammetric responses (sweep rate, 50 mV s^{-1}) recorded in a 0.5 M H_2SO_4 + 1 M CH_3OH solution at Pt/BDD (curve 1) and Pt/ TiO_2 /BDD (curve 2) electrodes with the same platinum loading. An increase of *ca.* 60% of the main peak current (at *ca.* 0.8 V) was observed when the Pt particles were deposited on the TiO_2 layer, compared to the case of the bare BDD support. We believe that this increase of the catalytic activity is mainly due to an enhanced active surface area of the electrocatalyst (which is the result of the good dispersion

photoinduced increase of *ca.* 25% of the peak current for methanol oxidation is an important result because it proves that hydrous titanium oxide obtained by simple electrochemical deposition on a suitable substrate could be used as a basis for obtaining new electrode materials with interesting electrochemical and photocatalytic properties.

The results obtained in this stage of the research were published in the following papers:

- Functional effects of the deposition substrate on the electrochemical behavior of platinum particles (Japanese Journal of Applied Physics 51 (2012) 090119-1-7.)
- Electrochemical preparation and characterization of a cobalt oxide-platinum composite with promising capacitive and electrocatalytic features (Journal of Solid State Electrochemistry 16 (2012) 3897-3905.)
- Electrocatalytic and photocatalytic activity of Pt–TiO₂ films on boron-doped diamond substrate (Applied Surface Science <http://dx.doi.org/10.1016/j.apsusc.2012.09.121>.)